Visible light communications: 3.75 Mbits/s data rate with a 160 kHz bandwidth organic photodetector and artificial neural network equalization [Invited]

Zabih Ghassemlooy,[1,*] Paul Anthony Haigh,[1,] Francesco Arca,[2] Sandro Francesco Tedde,[2,***] Oliver Hayden,[2] Ioannis Papakonstantinou,[3] and Sujan Rajbhandari[4]**

[1]*Optical Communications Research Group, Northumbria University, NE1 8ST, UK*
[2]*Siemens AG, Corporate Technology, Erlangen CT T DE HW3, Germany*
[3]*Department of Electronic & Electrical Engineering, University College London, WC1E 7JE, UK*
[4]*Department of Engineering Science, University of Oxford, OX1 3PJ, UK*
**Corresponding author: z.ghassemlooy@northumbria.ac.uk*
***Corresponding author: paul.haigh@northumbria.ac.uk*
****Corresponding author: sandro.tedde@siemens.com*

Received March 5, 2013; revised May 9, 2013; accepted May 10, 2013;
posted May 10, 2013 (Doc. ID 186399); published July 19, 2013

This paper presents an experimental demonstration of a visible light communications link with an light emitting diode and a low-bandwidth organic photodetector as transmitter and receiver, respectively, that achieves sub 4 Mbits/s speeds. An artificial neural network (ANN) equalizer is required in order to achieve such high data rates because of the influence of intersymbol interference. The digital modulation formats tested in this paper are non-return-to-zero on–off keying (OOK), and fourth-order pulse position modulation (4-PPM). Without equalization, data rates of 200 and 300 kbits/s can be achieved for 4-PPM and OOK, respectively. With ANN equalization, data rates of 2.8 and 3.75 Mbits/s can be achieved for the first time for OOK and 4-PPM, respectively.

OCIS codes: (060.4510) Optical communications; (250.2080) Polymer active devices.
http://dx.doi.org/10.1364/PRJ.1.000065

1. INTRODUCTION

Visible light communications (VLC) is an area for research that is picking up focus as an alternative to radio frequency (RF) technologies because of its bifunctionality, offering data communications and solid-state lighting, not to mention the ability to transmit data rates of 3.4 Gbits/s [1], which exceeds current commercial Wi-Fi technologies. Organic photodetectors (OPDs) are of interest for optical communications systems [2–5] due to advantages such as the possibility to fabricate the devices on flexible substrates and to achieve effortless large active area devices by using cost-effective processing techniques such as spray coating [6]. So far a megabit per second data rate has not been demonstrated in a wireless medium; however reports have emerged of organic optical communications in the fiber domain [3]. Here we report a data rate of 3.75 Mbits/s using a white phosphor light emitting diode (LED) as transmitter and an OPD as receiver.

OPDs are not expected to replace Si photodiodes in the near future in optical communications because of the latter's strong market position and wide user base. On the other hand, OPDs can be of interest for applications where Si photodiodes are not suitable and therefore are a really exciting technology for the future, also considering the significant cost reduction offered by spray coating at room temperature. Due to the low charge carrier mobility in organic semiconductors, which are orders of magnitude lower than in Si, the bandwidths (BWs) of OPDs are usually much lower than the BWs of Si devices, which is a major challenge.

The OPDs under test (produced under collaboration by Siemens AG Corporate Technology) are based on the bulk heterojunction principle [7]. Four diodes with 1 cm^2 active area each are fabricated on a single 5 cm × 5 cm transparent glass substrate as illustrated in Fig. 1.

The thin-film (~500 nm) organic semiconductor layer, a blend of poly-3-hexyl-thiophene (P3HT) as the donor material and [6,6]-phenyl C_{61} butyric acid methyl ester (PCBM) as the acceptor material, is deposited by spray coating from a xylene solution as in [6], which leads to extremely low-material-cost devices (~€0.20 cm^{-2}). This simple fabrication technique is extremely attractive for VLC systems. The OPD BW is dynamic and dependent on the incident light intensity ($W \cdot cm^{-2}$), as reported in [8]. In high light densities, the number of charge carriers is greater than the number of interface traps, and therefore the BW is proportional to the time constant of the plate capacitance. Conversely, in low light densities, the number of interface traps outnumbers the number of charge carriers; so the BW is proportional to the traps' time constant.

Further, the OPD is also attractive for VLC systems due to its superior responsivity compared to Si photodetectors in the visible range under a much smaller reverse bias, as shown in Fig. 2. It also has a sharp cutoff wavelength at ~620 nm due to the larger bandgap of P3HT (~2 eV) in comparison to Si (~1.16 eV). It should be noted that a bandgap of 2 eV is relatively high and has a cutoff wavelength around 620 nm (red wavelengths), which could be a problem for VLC applications

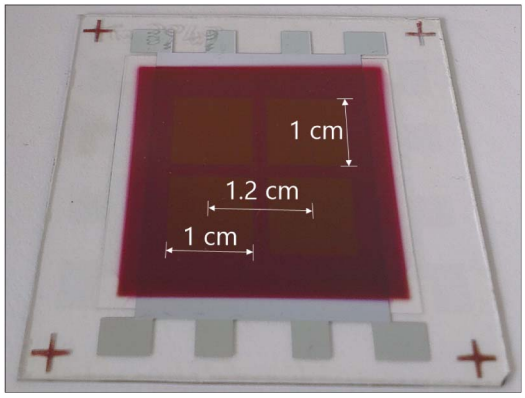

Fig. 1. Bottom view photograph of the OPD under test with spatial characteristics also noted.

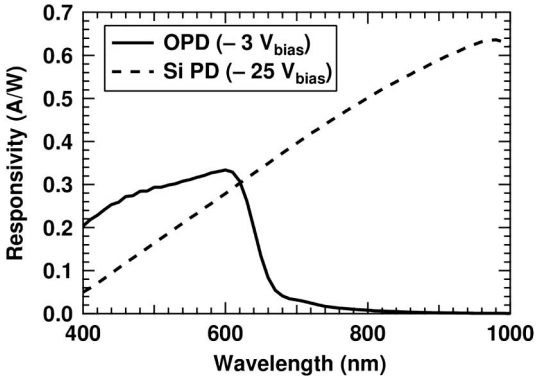

Fig. 2. Responsivity curves of the OPD under test and a generic ThorLabs PDA36A Si photodetector.

that take advantage of wavelength division multiplexing (WDM). The cutoff wavelength can be shifted to the near-infrared region by replacing P3HT in the bulk heterojunction blend with a low-bandgap material such as poly [2,6-(4,4-bis-(2-ethylhexyl)-4*H*-cyclopenta[2,1-b;3,4-b']dithiphene)-*alt*-4,7-(2,1,3-benzothiadiazole)] (PCPDTBT) as in [9].

In [4] a VLC link with the same composition of LED and OPD was proposed using the on–off keying (OOK) modulation format. The data rate reported was 750 kbits/s and required an artificial neural network (ANN)-based equalizer in order to recover the data. However, the light density on the OPD was not maximized, and a BW of 30 kHz was reported. Here we perform bit error rate (BER) measurements by varying the light densities between 10 and 300 $\mu W \cdot cm^{-2}$, obtaining BWs ranging between ~50 and 160 kHz. Furthermore, both OOK and fourth-order pulse position modulation (4-PPM) are investigated. 2-PPM is not examined because it has a higher spectral content around the DC and low frequencies regions while having the same BW requirements as 4-PPM. No higher orders of PPM are investigated because of the significant additional BW requirements. At the receiver an ANN equalizer is required in order to recover the data as in [4], since the required high data rates are much higher than the system BW.

2. TEST SETUP AND ARTIFICIAL NEURAL NETWORK

The test setup is shown in Fig. 3. The pseudorandom binary sequence in the OOK data format is generated in MATLAB

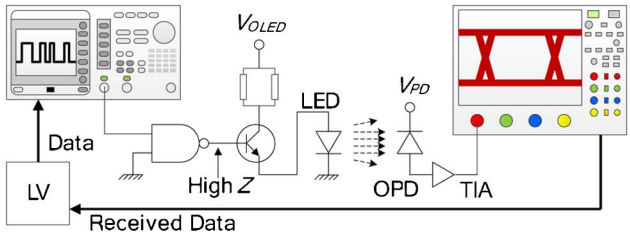

Fig. 3. Schematic system block diagram. TIA: transimpedance amplifier; V_{OLED}: LED bias voltage; V_{PD}: OPD bias voltage; High Z: high impedance.

and translated into the 4-PPM code. The data is output by a Tektronix AFG3022B function generation controlled by LabVIEW (LV in Fig. 3) and buffered by a NAND gate with a high output impedance, then mixed with a DC level prior to intensity modulation of the LED (Philips Luxeon Rebel, BW 4.4 MHz). The white light is transmitted over the linearly attenuating line-of-sight channel h as given by [10]

$$h(0) = \frac{A}{d^2} R_0(\theta) \cos(\varphi), \tag{1}$$

where A is the OPD active area (1 cm^2), d is the distance between the transmitter (LED) and receiver (OPD), θ is the angle of light emission, φ is the angle of incidence, and R_0 is the Lambertian radiation pattern of the LED, given by [10]

$$R_0(\theta) = \frac{m+1}{2\pi} \cos(\theta)^m, \tag{2}$$

where m is the Lambertian order.

At the receiver, the output of the photodetector is passed through an Analog Devices AD8015 (noise current density 2.4 $pA \cdot Hz^{-1/2}$) transimpedance amplifier, the output of which is acquired by an Agilent DSO9254A oscilloscope.

The OPD was reverse biased at –5 V as in [8] by using an Agilent 3631A controlled by LabVIEW. Then light was applied to the OPD through the transparent anode electrode. The applied light density was measured using an ~1 cm diameter thermopile disk (14BT, Laser Instrumentation Ltd). To yield insight into the OPD performance under different light densities, the applied light intensity was varied by varying the transmission (LED–OPD) distance. Incident light densities of 10, 50, 270, and 300 $\mu W \cdot cm^{-2}$ were generated and correspond to measured BWs of 56, 76, 110, and 160 kHz, respectively, as illustrated in Fig. 4. The BW difference between the lowest and the highest light density is ~100 kHz, which is a significant difference.

OOK is the most common modulation scheme for VLC systems due to its ease of implementation and BW efficiency [4]. Data are inferred by the presence or absence of a pulse of energy in the symbol period; see [11,12]. Conversely, PPM is the most power-efficient modulation scheme, requiring half the power of OOK at the expense of a twofold increase in the BW requirement that follows [13]:

$$\frac{P_{\mathrm{PPM}}}{P_{\mathrm{OOK}}} = \sqrt{\frac{2}{L \log_2 L}}, \tag{3}$$

where L is the order of PPM. This comes at the cost of decreased BW efficiency, following [13]

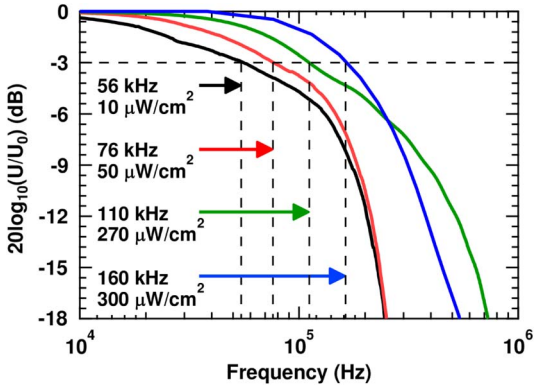

Fig. 4. OPD BWs for four light densities, varying from 10 to 300 $\mu W \cdot cm^{-2}$, corresponding to BWs ranging between 56 and 160 kHz, giving an ~100 kHz range.

$$\mathrm{BW}_{L\text{–PPM}} = \frac{LR_b}{\log_2 L}, \tag{4}$$

where R_b is the bit rate. The spectral signature of 4-PPM contains little or no DC and low-frequency components and thus is ideal for reducing the high-pass–filter-induced baseline wander phenomena that occurs in indoor optical wireless communication links [4]. Soft demodulation can also be used with 4-PPM, offering an electrical signal-to-noise ratio gain of more than 1.5 dB in the presence of signal distortion. Hence, threshold detection is not considered here for 4-PPM, since it will yield an inferior result [13].

Orthogonal frequency-division multiplexing is a popular option for increasing data rates in VLC systems, and extremely high data rates have been demonstrated. In order to really maximize the BW of such an orthogonal frequency-division multiplexing system, three equalizers are required; a preequalizer, a time domain equalizer, and a postequalizer. Each of these equalizers requires knowledge of the system and channel responses (as stated in [4]). So far no widely accepted feedback channel has been used in VLC systems, and therefore we prefer not to use such as a system, as it may not be viable in the future.

Instead, a high-performance equalizer such as the ANN can be used that does not require any knowledge of the channel because it acquires this information from a training sequence that consists of a known header file that is transmitted before the useful information. The multilayer perceptron (MLP) ANN is selected due to its superior performance in symbol error rate to transversal linear equalizers [14]. In theory, the MLP is not the optimal classifier; the decision feedback or radial basis function ANNs should outperform the MLP; however these configurations have a significantly higher computational intensity and complexity for only a slight increase in data rate [15]. The MLP consists of three layers; an input layer x, a hidden layer, and an output layer y with a single node. The N-input layer is the equivalent of an N-tap delay line in conventional filters; the number of nodes in the hidden layer is also made equal to N and is where the processing occurs. The output of the MLP is given by

$$y = f\left(b + \sum_i w_i x_i\right), \tag{5}$$

where $i = 0, \ldots, N$ if a bias b exists and $i = 1, \ldots, N$ otherwise. The filter weights are given by w_i and are adjusted during the ANN training in order to find the correct coefficients to map the system response.

The ANN is trained by the Levenberg–Marquardt backpropagation algorithm with an adaptive learning rate [16], which is supervised training that works on the basis of minimizing the error cost function E of a known bit sequence at the receiver and the transmitted data as follows [17]:

$$E(n) = \|y(n) - d(n)\|^2, \tag{6}$$

where d is the desired sample and y is the received sample. The backpropagation algorithm updates the weights as follows [17]:

$$w_{ij}(n+1) = w_{ij}(n) - \eta \frac{\partial E(n)}{\partial w_{ij}(n)}. \tag{7}$$

Once the ANN is fully trained, it can be used to correct the received data.

The ANN is capable of generalizing, which is another advantage over linear equalizers. This means that if an error occurs that the ANN was not trained for, the ANN has a higher probability of recovering the data than any other linear equalizer [17]. The ANN is implemented in MATLAB.

3. RESULTS

In Fig. 5 the BER performance for OOK using both threshold detection (denoted T/H) and the ANN equalizer is shown in high light density conditions with 160 kHz system BW. Furthermore the performance of 4-PPM with soft demodulation and the ANN equalizer is also shown. First considering the unequalized case, data rates of 500 and 300 kb/s can be achieved with 4-PPM and OOK, respectively, (1000 and 300 kHz BW requirement, respectively), showing that 4-PPM significantly outperforms OOK by offering an ~66% additional data rate.

The reason for this is attributed to the fact that soft demodulation depends on the signal gradient. As opposed to threshold detection, where the bit levels are assigned with reference to an average value, soft demodulation reshapes the incoming signal into an L-column matrix. The highest value is assigned a 1-level and the rest are assigned 0-levels. Failure of soft decoded 4-PPM is therefore caused by the rapid

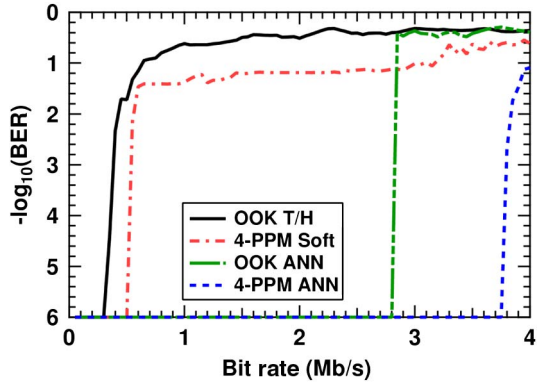

Fig. 5. BER performance for OOK and 4-PPM with and without ANN equalization.

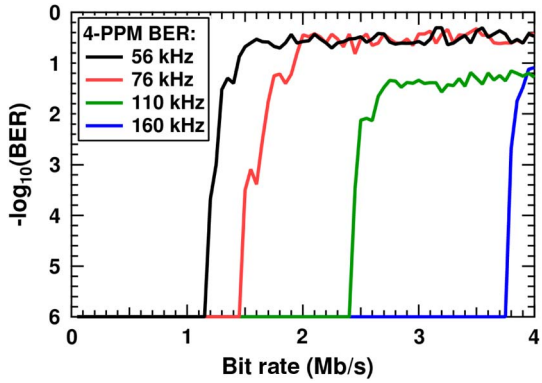

Fig. 6. BER performance of 4-PPM across the system with varying light density. In each case, over 1 Mbit/s can be supported.

transmission of alternative states where the transient response of the OPD is not sufficient and the signal gradient cannot become negative to be assigned a 0-level.

Considering the ANN equalizer performance, 4-PPM and OOK can offer 3.75 and 2.8 Mbits/s, respectively. As with the unequalized case, 4-PPM significantly outperforms OOK. Over ~1 Mbit/s extra data rate can be recovered with 4-PPM than OOK. The BW requirements are 7.5 and 2.8 MHz, respectively. The reason for the additional performance is that the ANN can easily differentiate between single pulses of energy followed by long streams of 0-levels in a highly multipath induced intersymbol-interference environment. However, in OOK each level is equiprobable, and there is therefore too much signal distortion to accurately estimate of the system response that is required for the ANN to undo the intersymbol-interference effect.

We have established that 4-PPM outperforms OOK in high light density conditions. Therefore now the BER performance of 4-PPM with the ANN equalizer is investigated over the four BWs (56, 76, 110, and 160 kHz) that are obtained by using four different light densities (10, 50, 270, and 300 $\mu W \cdot cm^{-2}$); see Fig. 6. The case of the 160 kHz BW has already been covered and can support 3.75 Mbits/s. Data rates up to 2.4, 1.45, and 1.15 Mbits/s can be supported for the BWs in descending order.

Each of the system BWs are separated by between ~20 and 40 kHz, and the performance decreases proportionally to the difference between them as expected. For example, there is a drop of 1.45 Mbits/s between the 160 and 110 kHz cases (40 kHz difference), which is significant. Furthermore there are drops of ~1 Mbits/s between the 110 and 76 kHz cases (34 kHz difference) while between 76 and 56 kHz the drop in data rate is only 0.3 Mbits (20 kHz). Therefore the performance is clearly related to the decrease in signal-to-noise ratio with decreasing light density and the increasing influence of intersymbol interference, thus making the data unrecoverable. Nevertheless, data rates >1 Mbits can be recovered across the entire system, which is an important result for OPD–VLC systems, as megahertz devices are starting to emerge [5] that could use this technology in order to provide high-speed and low-cost VLC systems.

4. CONCLUSION

In this paper we have experimentally demonstrated the first megabit per second VLC link with an OPD as receiver (to our knowledge). The modulation schemes tested were 4-PPM and OOK. We investigated the OPD performance under different light intensities that varied the OPD BW between 56 and 160 kHz. The ANN equalizer was used to maximize data rates up to 3.75 Mbits/s and 1 Mbit/s in high and low light densities cases, respectively, thus demonstrating the potential of large active area OPDs for optic-free VLC systems.

REFERENCES

1. G. Cossu, A. M. Khalid, P. Choudhury, R. Corsini, and E. Ciaramella, "3.4 Gbit/s visible optical wireless transmission based on RGB LED," Opt. Express **20**, B501–B506 (2012).
2. J. Clark and G. Lanzani, "Organic photonics for communications," Nat. Photonics **4**, 438–446 (2010).
3. M. Punke, S. Valouch, S. W. Kettlitz, M. Gerken, and U. Lemmer, "Optical data link employing organic light-emitting diodes and organic photodiodes as optoelectronic components," J. Lightwave Technol. **26**, 816–823 (2008).
4. P. A. Haigh, Z. Ghassemlooy, H. Le Minh, S. Rajbhandari, F. Arca, S. F. Tedde, O. Hayden, and I. Papakonstantinou, "Exploiting equalization techniques for improving data rates in organic optoelectronic devices for visible light communications," J. Lightwave Technol. **30**, 3081–3088 (2012).
5. W.-W. Tsai, Y.-C. Chao, E.-C. Chen, H.-W. Zan, H.-F. Meng, and C.-S. Hsu, "Increasing organic vertical carrier mobility for the application of high speed bilayered organic photodetector," Appl. Phys. Lett. **95**, 213308 (2009).
6. S. F. Tedde, J. Kern, T. Sterzl, J. Furst, P. Lugli, and O. Hayden, "Fully spray coated organic photodiodes," Nano Lett. **9**, 980–983 (2009).
7. C. J. Brabec, N. S. Sariciftci, and J. C. Hummelen, "Plastic solar cells," Adv. Funct. Mater. **11**, 15–26 (2001).
8. F. Arca, S. F. Tedde, M. Sramek, J. Rauh, P. Lugli, and O. Hayden, "Interface trap states in organic photodiodes," Sci. Rep. **3**, 1324 (2013).
9. C. Soci, I.-W. Hwang, C. Yang, D. Moses, Z. Zhu, D. Waller, R. Gaudiana, C. J. Brabec, and A. J. Heeger, "Charge carrier photogeneration and transport properties of a novel low-bandgap conjugated polymer for organic photovoltaics," Proc. SPIE **6334**, 63340D (2006).
10. J. M. Kahn and J. R. Barry, "Wireless infrared communications," Proc. IEEE **85**, 265–298 (1997).
11. J. G. Proakis, *Digital Communications* (McGraw-Hill, 2004).
12. Z. Ghassemlooy, W. Popoola, and S. Rajbhandari, *Optical Wireless Communications: System and Channel Modelling* (CRC Press, 2012).
13. S. Rajbhandari, Z. Ghassemlooy, and M. Angelova, "Bit error performance of diffuse indoor optical wireless channel pulse position modulation system employing artificial neural networks for channel equalization," IET Optoelectron. **3**, 169–179 (2009).
14. K. Hornik, M. Stinchcombe, and H. White, "Multilayer feedforward networks are universal approximators," Neural Netw. **2**, 359–366 (1989).
15. K. Burse, R. N. Yadav, and S. C. Shrivastava, "Channel equalization using neural networks: a review," IEEE Trans. Syst. Man. Cybernet. Part C Appl. Rev. **40**, 352–357 (2010).
16. L. Behera, S. Kumar, and A. Patnaik, "On adaptive learning rate that guarantees convergence in feedforward networks," IEEE Trans. Neural Netw. **17**, 1116–1125 (2006).
17. S. Haykin, *Neural Networks: A Comprehensive Foundation*, 2nd ed. (Prentice-Hall, 1998).